Title

Co/Pt Multilayers on Self-Organized Hexagonal Patterned Nanodots

Permalink

https://escholarship.org/uc/item/4qk4573z

Journal

IEEE Transactions on Magnetics, 50(11)

ISSN

0018-9464

Authors

Shi, Da Wei
Greene, Peter K
Liu, Pan
et al.

Publication Date

2014-11-01

DOI

10.1109/tmag.2014.2325647

Peer reviewed

Magnetic multilayers on self-organized hexagonal patterned nanodots

D. W. Shi [1], P. K. Greene [2], P. Liu [1], K. Javed [1], Kai Liu [2] and X. F. Han [1]*

[1]Beijing National Laboratory for Condensed Matter Physics, Institute of Physics, Chinese Academy of Sciences, Beijing 100190, China

[2]Physics Department, University of California, Davis, CA 95616 USA

Abstract- **Anodic alumina with surface of hexagonal patterned nanodots was prepared by a two-step anodizing procedure. SEM and AFM results clearly showed the formation of self-organized hexagonal patterned nanostructure. Diameters of the nanodots were controlled by choosing different anodization voltage and types of electrolyte acids. Co/Pt multilayers deposited on the nanodots with different diameters of 20, 70 and 100 nm lead to the formation of magnetic nanostructures with perpendicular anisotropy. Magnetometry and the first order reversal curve (FORC) method were used to study the magnetic properties of Co/Pt nanostructures. An out-of-plane magnetic easy axis was observed for the continuous films and the nanodots with the diameter of 100 and 70 nm. The magnetic multilayers deposited on 20 nm nanodots appeared to have taken on a "hard axis" type behavior. The curvature of nanodot arrays induces strong modifications on the magnetic properties of the nanostructures.**

Index Terms—**hexagonal patterned nanodots, magnetic multilayers, perpendicular magnetic anisotropy, first-order reversal curves**

I. INTRODUCTION

Extensive and increasing interest has been paid to the fabrication and investigation of materials at nanoscale [1-4]. Compared with their bulk counterparts, nanomaterials usually exhibit unique properties stemming from their nanoscale dimensions. Many of the functional nanomaterials have been demonstrated to have tremendous technological applications in the field of catalysts, sensors, biology, and magnetic recording devices [5-9]. Among them, potentials for ultrahigh-density magnetic recording media have excited much interests in patterned magnetic nanostructures [10-12]. Although lithographic techniques have been commonly employed to achieve arrays of isolated magnetic nanostructures, simple and inexpensive non-lithographic method of fabricating magnetic nanostructures has become increasingly important.

Recently, a new class of nanomaterial has been developed by using curved surfaces as substrate [13]. Magnetic multilayers deposited on self-organized pattern formed of spherical polystyrene (PS) nanoparticles results in tilted nanostructure material. There have been extensive studies on deposition of thin films on such colloidal nanosphere arrays [14-18]. However, like all organic compounds, polystyrene cannot be used for the deposition of materials under high temperature or for the post-annealing of the nanomaterials, which limits the variety of nanomaterials that can be fabricated. On the other hand, the self-organized formation of ordered hexagonal structures in anodic alumina has been used for the fabrication of various one-dimensional nanostructures such as nanowires, nanorods and nanotubes [19-21]. Porous magnetic nanostructures obtained by depositing magnetic thin films on porous anodized aluminum oxide (AAO) templates, commonly known as 'antidots', have also attracted a great deal of attention due to their potential applications as high-density magnetic data storage media [22-25]. Nonetheless the protuberant dot arrays at the bottom have long been ignored.

In this work, we report on the study of magnetic multilayers on self-organized hexagonal patterned nanodots. The semi-spherical nanodots were formed during electrochemical anodization of the ultra-pure aluminum foil. It can serve as another important alternative curved substrate for the exploration of nanomaterials.

II. EXPERIMENTAL METHOD

High purity (~99.999%) aluminum foils purchased from General Research Institute for Nonferrous Metals were used for electrochemical anodization. Prior to anodizing, they were first electropolished in 4:1 ratio by volume mixture of C_2H_5OH and $HClO_4$ to reduce the surface roughness. Standard two-step anodizing procedure in 0.3M oxalic acid solution at 0 °C was performed to get the aluminum oxide with a hexagonal patterned nanodots surface. Though the oxide barrier layer that closes the bottom ends of the pores was usually unwanted, after removal of the aluminum at the bottom, self-ordered nanoporous AAO templates were obtained. Here, the semi-spherical shaped barrier layer was used as curved substrate for the deposition of magnetic multilayers.

Magnetic multilayers with a structure of Pt (5 nm)/ [Co (0.5 nm)/Pt (1 nm)]$_4$/Co (0.5 nm)/Pt (5 nm) were deposited on the nanodots with diameters of 20, 70 and 100 nm by magnetron-sputtering. The angle between the direction of deposition and the substrate is about 30 °. The deposition rate of Co and Pt is 0.059 nm/s and 0.01 nm/s. The substrate was rotated during deposition. Continuous thin films with the same structure were deposited on the thermally oxidized Si wafer for comparison.

The morphologies of the nanodot arrays were characterized by scanning electron microscope (SEM) and atomic force microscopy (AFM). Magnetic properties of the Co/Pt nanostructures have been measured by a vibrating sample magnetometer (VSM) at room temperature.

III. RESULTS AND DISCUSSION

Fig. 1 shows the synthesis procedure of anodic alumina with protuberant dot arrays at the bottom schematically. Ordered semi-spherical nanopits surface was formed after the first step anodization. These nanopits led to the formation of hexagonal pore arrays in anodic alumina. It should be noted that the nanopits may be used to create novel nanostructure arrays as well. The leftover aluminum after the second anodization step was removed, and hexagonal patterned nanodot arrays were obtained. Oxalic, sulfuric and phosphoric acids can be used to fabricate AAO template with different pore diameters [26, 27]. However, oxalic acid is the most common choice. Thus the anodization voltage becomes the primary controllable factor for the diameter of the nanostructures. The relationship between the pore diameter and the anodization voltage is correlated with a voltage dependence of the volume expansion of the aluminum during oxidation and the current efficiency for oxide formation. In this work, nanodots with diameters of 20, 70 and 100 nm were used for further investigation.

Magnetic multilayers with the same structure of Pt (5 nm)/ [Co (0.5 nm)/Pt (1 nm)]$_4$/Co (0.5 nm) was coated on the nanodots and the thermally oxidized Si wafer by magnetron-sputtering method. An additional 5 nm Pt layer was deposited to avoid oxidation. The structure and morphology of typical nanodot arrays with different diameters after sputtering are illustrated in Fig. 2. The AFM images clearly show that all of the three samples still maintain a hexagonal patterned nanostructure. The cross section analysis before and after deposition of Co/Pt multilayers shows the geometry of the dots. The depth between dots increases slightly after deposition of the multilayers. It should be pointed out that the total thickness of the magnetic stack is comparable to the height of the 20 nm nanodots. The formation of ordered magnetic caps was attributed to the deposition conditions in our sputtering system. The Co and Pt targets were off axis and tilted, and the substrate was rotating during deposition resulting in a strong shadowing effect. Thus only very little material is deposited around the edges of the nanodots.

Magnetic properties of Co/Pt multilayers deposited on the hexagonal patterned nanodots were also characterized. Magnetometry and the first-order reversal curves (FORC's) were measured with the field perpendicular to the substrate surface. The observed square shaped loops when the magnetic field was perpendicular to the films show an out-of-plane magnetic easy axis for the continuous films. Compared with the hysteresis loop of the continuous film, hysteresis loops of the exchange bias nanostructures were much more sheared due to the increase of disorder disrupting reversal as the size of the nanodots become smaller.

The FORC method has proven to be a powerful method to provide detailed information on the magnetization reversal of a large variety of magnetic systems [28-31]. For each FORC, the sample is brought from positive saturation to a reversal field H_r, then the magnetization is measured under increasing applied field H_a. A FORC-distribution is then extracted according to

$$\rho(H_a, H_r) = -\frac{1}{2}\frac{\partial^2 M(H_a, H_r)}{\partial H_a \partial H_r} \qquad (1)$$

The FORC distribution eliminates purely reversible

components of the magnetization switching [28, 32]. It maps the reversal events in terms of local coercive field $H_c = (H_a - H_r)/2$ and interaction field $H_b = (H_a + H_r)/2$. In the case of continuous flat thin films, magnetization reversal usually proceeds by domain nucleation and propagation [28]. For the multilayers deposited on the nanodots, since exchange coupling across individual nanocaps is somewhat impeded, each nanocap will reverse its magnetization almost independently, more so for the smaller nanodot sizes. An enhancement in H_c values respect the continuous film was observed for the 70 nm and 100 nm nanodots. Similar results have been studies by depositing on the nanoparticles with different diameter [33]. The dipole-dipole interaction between the neighboring nanocaps plays an important role in the enhancement of coercivity. Another reason for the increase of the coercivity is the pinning effect caused by the morphology of the nanodot arrays. High coercivity tail in the FORC distributions is apparent for both 70 nm and 20 nm samples (Figs. 3b and 3c), also suggesting that domain wall pinning is enhanced as the dot size decreases. For 100 nm dots, the vertical ridge in the FORC distribution (Fig. 3a) indicates the existence of strong demagnetizing dipolar interactions [30, 31], consistent with perpendicular anisotropy in the patterned Co/Pt. This vertical ridge diminishes in 70nm sized dots (Fig. 3b), as the perpendicular anisotropy decreases. Finally in the 20nm sized dots, the FORC distribution is much broader (Fig. 3c) due to a relatively higher degree of disorders [24, 34]. We also observed an abnormal drop in coercivity for the 20 nm sized sample. As the thickness of Co/Pt multilayer approaches the nanosphere diameter, neighboring nanocaps are interconnected, and the multilayer transitions from isolated nanocaps to interconnected caps which is similar to the continuous film.

To further understand the magnetization reversal process of Co/Pt nanostructures, magnetic hysteresis loops and angular dependence of remanent squareness (SQ) are shown in Fig. 4. Series of magnetization hysteresis loops of the Co/Pt nanostructures with different angles between the surface of the substrate and the external field have been measured. When the angle is 0 °, the magnetic field is applied parallel to the substrate surface; and when the angle is 90 °, the external magnetic field is perpendicular to the substrate. Fig. 4(a), (b) and (c) show the magnetization hysteresis loops of the Co/Pt multilayer deposited on 20 nm, 70 nm and 100 nm nanodots respectively. For the 70 nm and 100 nm nanostructures, the magnetization hysteresis loop becomes more compressed with the decrease of the angle. To the contrary, the magnetic multilayers deposited on 20 nm nanodots shows an opposite trend. It can be noted from Fig 4(d) that squareness (SQ) values for three cases (20 nm, 70 nm, and 100 nm dots) show different tendency with increasing angle. Highest value was detected at 90 ° for the 70 nm and 100 nm nanodots which is the magnetic easy axis of the arrays. The "hard axis" type behavior for the 20 nm nanodots when the magnetic field was applied perpendicular to the substrate surface was further confirmed here.

IV. CONCLUSION

In summary, the semi-spherical nanodots at the bottom formed during electrochemical anodization of the ultra-pure

aluminum foil was demonstrated to be another important alternative curved substrate for the exploration of nanomaterials. Co/Pt multilayers were deposited on the self-organized hexagonal patterned nanodots with different diameters. The curved surface still maintains a hexagonal patterned nanostructure even when the total thickness of the magnetic stack is comparable to the height of the nanodots due to the shadowing effect. Increasing coercivity with the decrease of the nanodot size was observed compared with the flat films. An abnormal drop of coercivity for the multilayers deposited on 20 nm nanodots was observed. Both the dipole-dipole interaction between the neighboring nanocaps and the disorder disruption can strongly affect the magnetic reversal process of the nanostructures. The curvature of the protuberant dot arrays induces strong modifications in the magnetic properties, which is interesting both for technical applications and fundamental studies.

REFERENCES

[1] A. Thess, R. Lee, P. Nikolaev, H. J. Dai, P. Petit, J. Robert, C. H. Xu, Y. H. Lee, S. G. Kim, A. G. Rinzler, D. T. Colbert, G. E. Scuseria, D. Tománek, J. E. Fischer, R. E. Smalley, "Crystalline Ropes of Metallic Carbon Nanotubes," *Science*, vol. 273, pp. 483-487, July.1996.

[2] S. Iijima, "Helical microtubules of graphitic carbon," *Nature.*, vol. 254, pp.57-58, Nov. 1991

[3] J. L.Lauhon, M. S. Gudiksen, D. Wang, C. M. Lieber, "Epitaxial core–shell and core–multishell nanowire heterostructures," *Nature.*, vol. 420, pp. 57–61, Sep. 2002.

[4] D. Moore, J. R. Morber, R. L. Snyder, Z. L.Wang, "Growth of Ultralong ZnS/SiO$_2$ Core-Shell Nanowires by Volume and Surface Diffusion VLS Process," *J. Phys. Chem. C*, vol. 112, pp. 2895-2903, Dec. 2007.

[5] H. Dai, J. H. Hafner, A. G. Rinzler, D. T. Colbert, and R. E. Smalley, "Nanotubes as nanoprobes in scanning probe microscopy," *Nature,* vol. 384, pp. 147-150, Nov. 1996.

[6] X. Kou, X. Fan, H. Zhu and J. Q. Xiao, "Tunable ferromagnetic resonance in NiFe nanowires with strong magnetostatic interaction," *Appl. Phys. Lett.,* vol. 94, p. 112509, Mar. 2009.

[7] A. Kros, R. J. M. Nolte, and N. A. J. M. Sommerdijk, "Conducting Polymers with Confined Dimensions: Track-Etch Membranes for Amperometric Biosensor Applications," *Adv. Mater.*, vol. 14, pp. 1779-1782, Nov. 2002

[8] C. A. Haberzettl, "Nanomedicine: destination or journey?" *Nanotechnology,* vol. 13, pp. R9-R13, Oct. 2002

[9] R. K. Dumas, C. P. Li, I. V. Roshchin, I. K. Schuller and K. Liu, "Deconvoluting reversal modes in exchange-biased nanodots," *Phys. Rev. B*, vol. 86, p. 144410, Oct. 2012.

[10] A. Yu. Toporov, R. M. Langford and A. K. Petford-Long, "Lorentz transmission electron microscopy of focused ion beam patterned magnetic antidot arrays," *Appl. Phys. Lett.*, vol. 77, p. 3063, Sept. 2000.

[11] Stephen Y. Chou, "Patterned magnetic nanostructures and quantized magnetic disks," *PROCEEDINGS OF THE IEEE*, vol. 85, pp. 652-670, Apr. 1997.

[12] A. O. Adeyeye and N. Singh, "Large area patterned magnetic nanostructures," *J. Phys. D: Appl. Phys.* vol. 41, p. 153001, July 2008.

[13] M. Albercht, G. H. Hu, I. L. Guhr, T. C. Ulbrich, J. Boneberg, P. Leiderer and G. Schatz, "Magnetic multilayers on nanospheres," *Nat. Mater,* vol. 4, pp. 203-206, Mar.2005.

[14] S. M. Yang, S. G. Jang, D. G. Choi, S. Kim, H. K. Yu, "Nanomachining by Colloidal Lithography," *Small.*, vol. 2, pp. 458, Mar. 2006.

[15] C. L. Cheung, R. J. Nikolić, C. E. Reinhardt and T. F. Wang, "Fabrication of nanopillars by nanosphere lithography," *Nanotechnology,* vol. 17, pp. 1339–1343, Feb. 2006.

[16] T. C. Ulbrich, D. Makarov, G. Hu, I. L. Guhr, D. Suess, T. Schrefl, and M. Albrecht, "Magnetization Reversal in a Novel Gradient Nanomaterial," *Phys. Rev. Lett.*, vol. 96, p. 077202, 2006.

[17] A. Plettl, F. Enderle, M. Saitner, A. Manzke, C. Pfahler, S. Wiedemann and P. Ziemann, "Non-Close-Packed Crystals from Self-Assembled Polystyrene Spheres by Isotropic Plasma Etching: Adding Flexibility to Colloid Lithography," *Adv. Func. Mater.* vol. 19, pp. 3279-3284, Aug. 2009.

[18] R. Brandt, R. Ruckriem, D. A. Gilbert, F. Ganss, T. Senn, Kai Liu, M. Albrecht, and H. Schmidt, "Size-dependent magnetization switching characteristics and spin wave modes of FePt nanostructures", *J. Appl. Phys.* Vol. 113, p. 203910, May 2013.

[19] F. F. Tao, M. Y. Guan, Y. Jiang, J. M. Zhu, Z. Xu, and Z. Xue,, "An Easy Way to Construct an Ordered Array of Nickel Nanotubes: The Triblock-Copolymer-Assisted Hard-Template Method," *Adv.. Mater.* vol. 78, pp. 2161-2164, July 2006.

[20] X. F. Han, S. Shamaila, R. Sharif, J. Y. Chen, H. R. Liu, and D. P. Liu, "Structural and Magnetic Properties of Various Ferromagnetic Nanotubes," *Adv.. Mater.* vol. 21, pp. 4619-4624, Dec. 2006.

[21] J. Y. Chen, H. R. Liu, N. Ahmad, Y. L. Li, Z. Y. Chen, W. P. Zhou, and X. F. Han, "Effect of external magnetic field on magnetic properties of Co–Pt nanotubes and nanowires," *J. Appl. Phys.*, vol. 109, p. 07E157, Apr. 2011.

[22] K. Liu and C. L. Chien, "Magnetic and magneto-transport properties of novel nanostructured networks", *IEEE Trans. Magn.*, vol. 34, pp. 1021-1023, July 1998.

[23] M. T. Rahman, N. N. Shams, Y. C. Wu, C. H. Lai and D. Suess, "Magnetic multilayers on porous anodized alumina for percolated perpendicular media," *Appl. Phys. Lett.*, vol. 91, p. 132505, Sept. 2007.

[24] M. T. Rahman, Randy K. Dumas, Nasim Eibagi, Nazmun N. Shams, Yun-Chung Wu, K. Liu, and C. H. Lai, "Controlling magnetization reversal in Co/Pt nanostructures with perpendicular anisotropy", *Appl. Phys. Lett.*, vol. 94, p. 042507, Jan. 2009.

[25] W. J. Gong, W. J. Yu, W. Liu, S. Guo, S. Ma, J. N. Feng, B. Li, and Z. D. Zhang, "Exchange bias and its thermal stability in ferromagnetic/antiferromagnetic antidot arrays," *Appl. Phys. Lett.*, vol. 101, p. 012407, July 2012.

[26] O. Jessensky, F. Mü̈ller, and U. Gö̈sele, "Self-organized formation of hexagonal pore arrays in anodic alumina," *Appl. Phys. Lett.*, vol. 72, p. 1773, Mar. 1998.

[27] J. P. Zhang, J. E. Kielbasa, David L. Carroll, "Controllable fabrication of porous alumina templates for nanostructures synthesis," *Materials Chemistry and Physics,* vol. 122, pp. 295-300, Feb. 2010.

[28] J. E. Davies, O. Hellwig, E. E. Fullerton, G. Denbeaux, J. B. Kortright and Kai Liu, "Magnetization reversal of Co/Pt multilayers: microscopic origin of high field magnetic irreversibility", *Phys. Rev. B*, vol. 70, p. 224434, Dec. 2004.

[29] R. K. Dumas, Kai Liu, C. P. Li, I. V. Roshchin, and I. K. Schuller, "Temperature Induced Single Domain - Vortex State Transition in sub-100nm Fe Nanodots", *Appl. Phys. Lett. vol.* 91, p. 202501, Nov. 2007.

[30] X. M. Kou, X. Fan, R. K. Dumas, Q. Lu, Y. P. Zhang, H. Zhu, X. K. Zhang, Kai Liu, and J. Q. Xiao, "Memory effect in magnetic nanowire arrays," *Adv.. Mater.* vol. 23, p. 1393, Mar. 2011.

[31] D. A. Gilbert, G. T. Zimanyi, R. K. Dumas, M. Winklhofer, A. Gomez, N. Eibagi, J. L. Vicent and K. Liu, "Quantitative Decoding of Interactions in Tunable Nanomagnet Arrays Using First Order Reversal Curves," *Scientific Reports*, vol. 4, p. 4204, Feb. 2014.

[32] I. D. Mayergoyz, *Mathematical Models of Hysteresis* (Springer-Verlag, New York, 1991).

[33] Y. J. Zhang, W. Li, J. Li, Y. M. Zhang, Y. X. Wang, S. Y. Yang, S. S. Liu, L. C. Wu, Geoffrey S. D. Beach and J. H. Yang, "Perpendicular exchange bias of [Pt/Co]n/CoO multilayer on ordered nanosphere arrays," *J. Appl. Phys.*, vol. 111, p. 053925, Mar. 2012.

[34] M. S. Pierce, C. R. Buechler, L.B. Sorensen, S.D. Kevan, E.A. Jagla, J.M. Deutsch, T. Mai, O. Narayan, J. E. Davies, Kai Liu, G.T. Zimanyi, H. G.

Katzberger, O. Hellwig, E. E. Fullerton, P. Fischer, and J. B. Kortright, "Disorder induced magnetic memory: Experiments and theories", *Phys. Rev. B*, vol. 75, p. 144406, Apr. 2007.
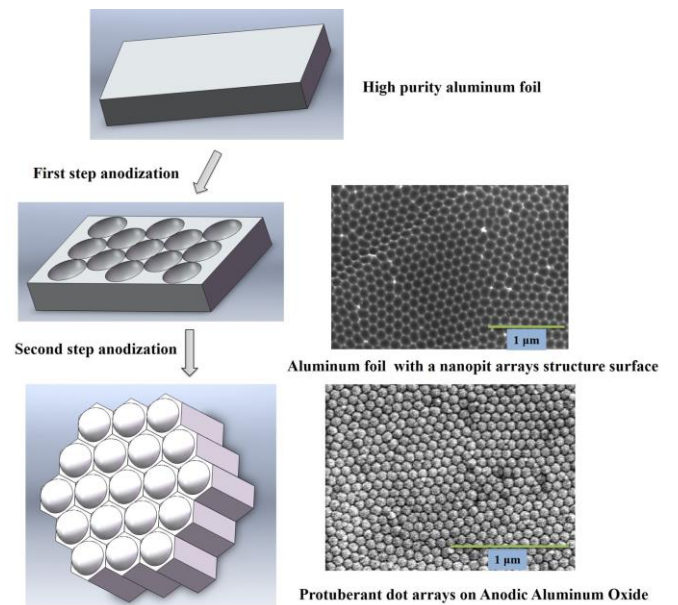

Fig. 1. The synthesis procedure of the anodic alumina with protuberant dot arrays: standard two-step anodizing procedure in 0.3M oxalic acid solution at 0 °C. SEM show the formation of semi-spherical nanopits and hexagonal patterned nanodot arrays.
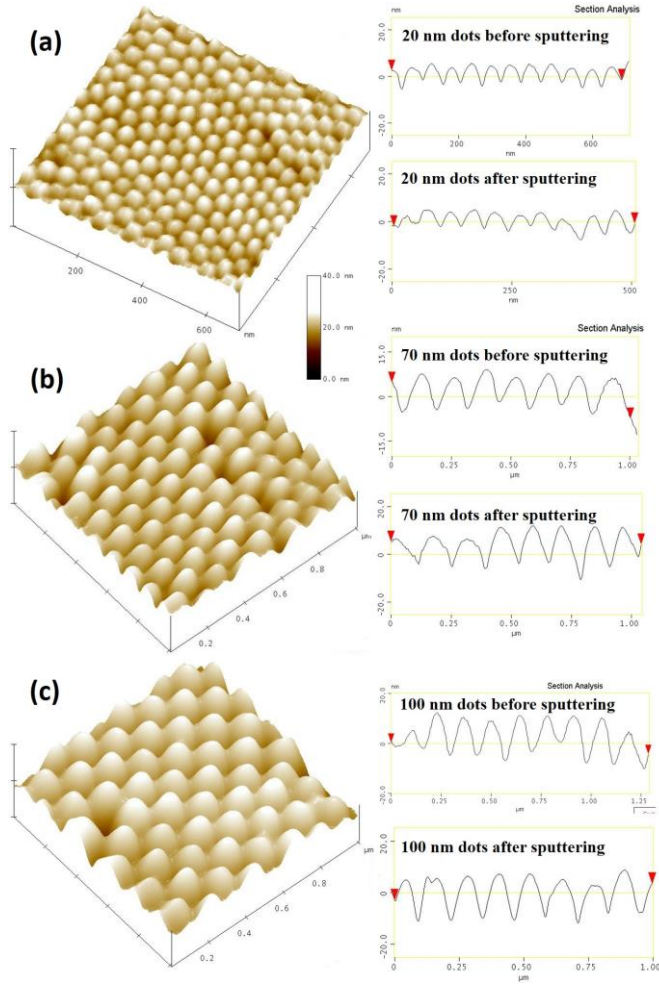
Fig. 2. Typical AFM images of the nanodot arrays with different diameters: (a) 20 nm; (b) 70 nm; (c) 100 nm, after deposited with Co/Pt multilayers with a structure of Pt (5 nm)/ [Co (0.5 nm)/Pt (1 nm)]$_4$/Co (0.5 nm)/Pt (5 nm). Cross section of the nanodots before and after Co/Pt multilayers deposition shows the geometry of the dots
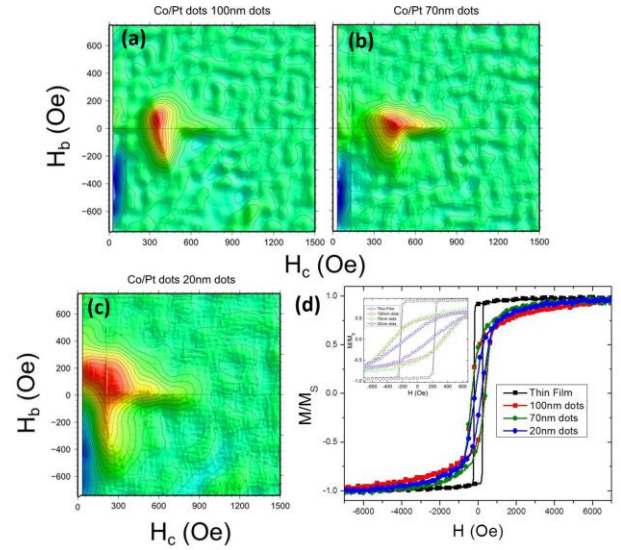

Fig. 3. FORC distributionsof Co/Pt multilayers deposited on different substrates: (a) 100 nm dots; (b) 70 nm dots; (c) 20 nm dots; (d) M-H loops of continuous film and nanodots with different diameters, which are measured with VSM in the out of plane geometry. The inset shows the corresponding enlarged M(H) loops.
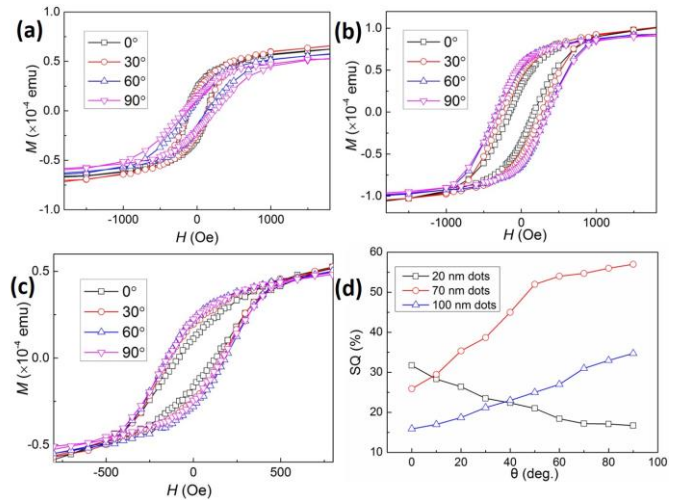

Fig. 4. Magnetic hysteresis loops and angular dependence of remanent squareness (SQ) for Co/Pt deposited on (a) 20nm, (b) 70nm, and (c) 100nm nanodots. A summary is shown in (d).